Fibers and Polymers 2013, Vol.14, No.12, 1985-1992 DOI 10.1007/s12221-013-1985-3

Antibacterial Effect of Carbon Nanofibers Containing Ag Nanoparticles

Hany S. Abdo[1,2], Khalil Abdelrazek Khalil[1,2]*, Salem S. Al-Deyab[3], Hamoud Altaleb[3], and El-Sayed M. Sherif[4,5]

[1]*Mechanical Engineering Department, College of Engineering, King Saud University, Riyadh 11421, Saudi Arabia*
[2]*Mechanical Design and Materials Department, Faculty of Energy Engineering, Aswan University, Aswan, Egypt*
[3]*Department of Chemistry, King Saud University, Riyadh 11451, Saudi Arabia*
[4]*Center of Excellence for Research in Engineering Materials (CEREM), College of Engineering, King Saud University, Al-Riyadh 11421, Saudi Arabia*
[5]*Electrochemistry and Corrosion Laboratory, Department of Physical Chemistry, National Research Centre (NRC), Dokki, 12622 Cairo, Egypt*

(Received April 10, 2013; Revised July 10, 2013; Accepted July 19, 2013)

Abstract: Silver nanoparticles imbedded in polyacrylonitrile (PAN) nanofibers and converted into carbon nanofibers by calcination was obtained in a simple three-step process. The first step involves conversion of silver ions to metallic silver nanoparticles, through reduction of silver nitrate with dilute solution of PAN. The second step involves electrospinning of viscous PAN solution containing silver nanoparticles, thus obtaining PAN nanofibers containing silver nanoparticles. The third step was converting PAN/Ag composites into carbon nanofibers containing silver nanoparticles. Scanning electron microscopy (SEM) revealed that the diameter of the nanofibers ranged between 200 and 800 nm. Transmission electron microscopy (TEM) and energy dispersive spectroscopy (EDS) showed silver nanoparticles dispersed on the surface of the carbon nanofibers. The obtained fiber was fully characterized by measuring and comparing the FTIR spectra and thermogravimetric analysis (TGA) diagrams of PAN nanofiber with and without imbedded silver nanoparticles, in order to show the effect of silver nanoparticles on the electrospun fiber properties. The obtained carbon/Ag composites were tested as gram-class-independent antibacterial agent. The electrosorption of different salt solutions with the fabricated carbon/Ag composite film electrodes was studied.

Keywords: Carbon nanofiber, Electrospun, Silver nanoparticle, Water purification, Antibacterial effect

Introduction

Silver nanoparticles play a major role in the emerging field of nanotechnology in the past two decades. Colloidal silver is of particular interest because of its valuable application in life science as biosensors, labels for cells and bio-molecules, peptide probes, anti-microbial agents, wound healing agent and cancer therapeutics. The exciting and most important application of silver nanoparticles is its prominent anti-microbial activity [1-9]. Polyacrylonitrile (PAN), a well-known polymer with good stability and mechanical properties, has been widely used in producing carbon nanofibers (CNFs) as these have attracted much recent attention due to their excellent characteristics, such as spinnability, environmentally benign nature and commercial viability. Among the various precursors to produce CNFs, PAN has been extensively studied due to its high carbon yield and flexibility for tailoring the structure of the final CNFs as well as the ease of obtaining stabilized products due to the formation of a ladder structure via nitrile polymerization. In view of this, they have applications in areas such as electronics, tissue engineering, membrane filtration and high performance composites [5-7,10-19].

Adding metal nanoparticles to polymer nanofiber matrix (metal-polymer nanocomposites) has attracted a great attention due to synergic combinations of the unique optical, electrical, and catalytic properties of metal nanoparticles and excellent specific surface area of polymer nanofibers [1-8]. The incorporation of Ag nanoparticles into polyacrylonitrile (PAN) fibers exhibits excellent catalytic activity, surface-enhanced Raman scattering activity, electrical conductivity, and antimicrobial activity [2,5,6]. PAN is reported to be an important engineering polymer that has been widely used to produce a variety of synthetic fibers [2,20-33]. Zhang *et al.* [2] and Wang *et al.* [3] were succeeded to synthesis well dispersed Ag nanoparticles on the surface of the PAN nanofiber, but their method is critical in preventing nanoparticles from aggregation. Where conventional methods prepared by mechanical mixing the metal nanoparticles into dissolved polymer matrix leads to homogeneous dispersion of particles especially in the low viscous matrix [34-39].

In this paper, in situ preparation of silver nanoparticles mixed homogeneously in PAN solution to produce nanofiber film spun by electrospinning technique has been presented. Electrospinning is a process by which a suspended droplet of polymer solution is charged to high voltage to produce fibers with diameters ranging from 200 to 500 nm. When a voltage is sufficient to overcome surface tension forces, fine jets of liquid shoot out toward a grounded collector. The jet is stretched and elongated before it reaches the collector, dries and is collected as an interconnected film of nanofibers. This novel nanofiber spinning technique has been explored mainly

*Corresponding author: kabdelmawgoud@ksu.edu.sa

to prepare pure polymer nanofibers in past years [40-47]. We present a convenient and effective way to add Ag nanoparticles into PAN nanofiber film. UV spectrum and TEM studies have been done in order to reveal the structural properties of the Ag/PAN nanocomposite film.

Experimental

Materials

PAN was prepared with a redox system in aqueous solution (precipitation polymerization). The procedure can be summarized as following; In 250 m*l* round-bottomed flask, acrylonitrile (AN) (I) (15 m*l*, 230.30 mmol) was mixed with distilled water (175 m*l*) at room temperature with stirring under nitrogen atmosphere. Then, sodium disulfite solution (5 %, 0.5 m*l*, 0.13 mmol) and ferrous sulfate solution (2.5 m*l*, 9.10 mmol), were added followed by potassium proxodisulfate solution (5 %, 2.5 m*l*, 0.46 mmol). The turbidity was noted after 5 min and stirring was continuing for more 20 min. The precipitated polymer was flittered and was washed with distilled water (300 m*l*) and then finally washed with methanol (100 m*l*). The product was dried in oven under vacuum at 50 °C overnight to yield 7.9 g (65.83 % yields).

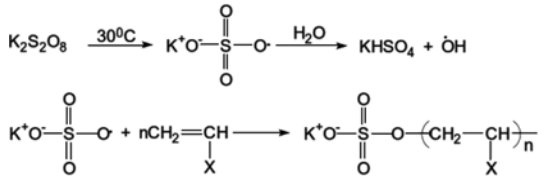

Preparation of PAN Nanofiber Film by Electrospinning

PANNF film was prepared by electrospinning (Figure 1). PAN (5 wt.%) was dissolved in DMF, and stirred until homogenous at room temperature. After that, the solution obtained was added into a plastic syringe, the internal diameter of plastic was 20 cm, the pinhead was connected to a 20-kV high-voltage, and aluminum foil served as counter electrode. The distance between the capillary and electrode was 21 cm, the feed rate of the solution was adjusted to 0.1 m*l*/h through a syringe pump. The electrospinning was performed at room temperature.

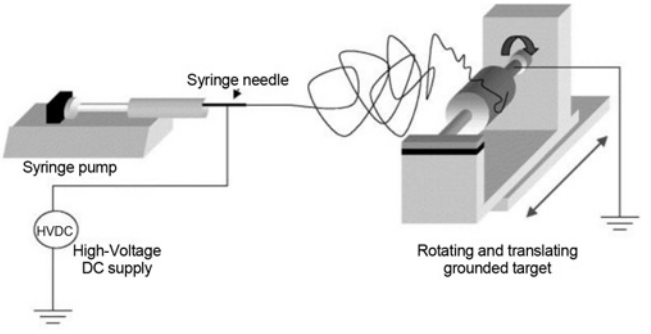

Figure 1. Schematic for electrospinning system.

Preparation of PAN Solution Containing Ag Particles

0.03 mg $AgNO_3$ (99.99 %, Sigma-Aldrich Co., USA) dissolved in 70 m*l* DMF with stirring at 30 min (the weight percentage of $AgNO_3$ in the solution and the time of stirring for optimum reduction was investigated by UV/vis spectrometer), 5 wt % PAN was then added to the solutions followed by stirring for 24 h at room temperature. The solution obtained was added into a plastic syringe with 20 mm internal diameter and 0.5 mm needle, the pinhead was connected to a (20 kV) high-voltage, and aluminum foil served as counter electrode. The distance between the capillary and electrode was 21 cm. the feed rate of the solution was adjusted to (0.1, 0.2, 0.3 and 0.4 m*l*/h) through a syringe pump. The electrospinning was performed at room temperature.

Treatment of PAN/Ag Composite Nanofiber (Stabilization, Carbonization)

The PAN/Ag nanofibers were stabilized in an air atmosphere at 270 °C for 2 h (at a heating rate of 2 °C/min) and followed by carbonization at 600, 650, 700, 750, 1000 °C for 1 h (at a heating rate of 4.5 °C/min) under an inert nitrogen atmosphere to yield carbonized. Stabilization is necessary to form a ladder structure that can withstand high temperatures during carbonization. During stabilization and carbonization, calcination of Ag also occurs and it is important because it increases the crystallinity of the nanoparticles which enhances photocatalytic activity. Using a programmable tube furnace, the nanofibers mats produced from electrospinning were heated at a rate of 2 °C/min up to 270 °C and maintained at this temperature for 2 hours (Figure 2). After the stabilization process, nitrogen gas was purged into the furnace to remove unwanted air or oxygen. This was done to prevent oxidation of fibers at high temperatures. The nanofibers were then heated at a rate of 4.5 °C/min up to 600, 650, 700, 750, 1000 °C in a nitrogen environment. The resulting carbon nanofibres were cooled down to room temperature in an inert gas atmosphere before

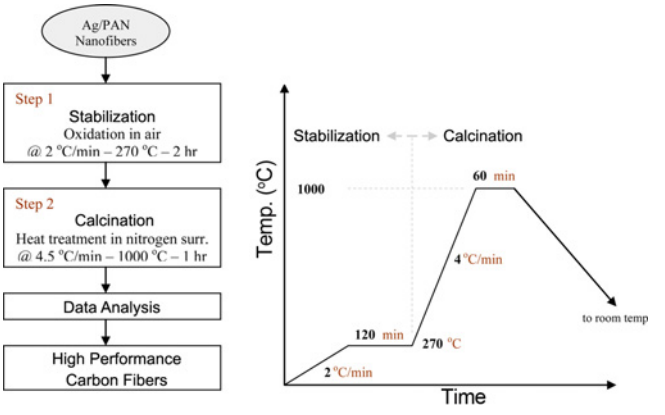

Figure 2. Stabilization and carbonization processes.

they were taken out of the furnace.

Antibacterial Assay Using the Disc Diffusion Method

Microorganisms used for the experiment are from the Microbiological Department, King Saud University University: *E.coli* o157:H7 ATCC 51659, *Staphylococcus aureus* ATCC 13565, Bacillus cereus EMCC 1080, *Listeria monocytogenes* EMCC 1875 and *Salmonella typhimurium* ATCC25566. Screening of different samples (4 discs samples in 5 mm diameter) was tested by disc diffusion method. Each sample (0.5 cm in diameter) was inoculation on Tryptose soy agar supplement with yeast extract (TSAYE) in a standard Petri dish from a 16-18 h culture grown in TSAYE broth inoculums were incubated at 37 °C. The concentration of bacteria inoculated in TSAYE was 2×10^6 cfu/m*l*. All experiments were performed in duplicate. The inhibition zone diameter was measured and expressed in millimeters.

Results and Discussion

Polymerization of Acrylonitrile

The use of polymers to prevent agglomeration and to obtain good dispersion in solution is quite well known [5]. Figure 3(a) illustrates the UV absorption spectra of the prepared PAN/Ag solution for different $AgNO_3$ concentrations. It was seen that the absorption band was centered at 450 nm wavelength which was typical for the formation of Ag^0 in the solution. To study the effect of $AgNO_3$ concentration, a 0.0025, 0.005, 0.01, 0.03, 0.05 and 0.1 grams of $AgNO_3$ were dissolved in 70 m*l* of DMF then 0.01 gm of polyethylene glycol was added as stabilizer and reduction agent. This solution was stirred for 30 min before analyze using UV spectra. While the influence of stirring time on UV absorption spectra for the prepared PAN/Ag solution can be construed from the results shown in Figure 3(b). Furthermore, the effect of stirring time has also been studied. The best concentration from the previous step (0.03 gm of $AgNO_3$ dissolved in 70 m*l* DMF) was prepared with stirring during 3 hours and result taken every 15 min by UV spectra. Noticeable changes in the UV absorption spectra were first observed for the solutions that had been sintered for at least 15 minutes. Regardless of the initial $AgNO_3$ concentration, an increase in the sintering time resulted in a monotonous increase in the intensity of the surface. Plasmon band centering around 420-430 nm, which reached a maximum value at about 3 hours of sintering.

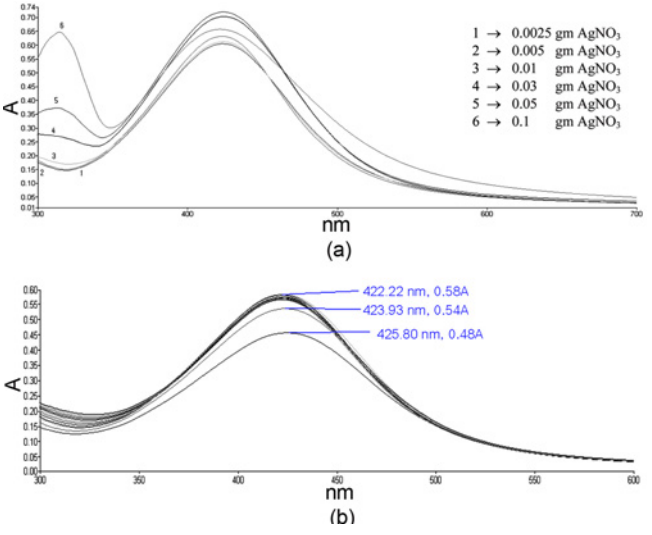

Figure 3. (a) Effect of $AgNO_3$ concentration and (b) effect of stirring time.

Electrospinning of PAN/Ag Fibers

Metal ions and metal compounds have been extensively studied in various fields like antimicrobial filters, wound dressing material, water disinfection, sensors, chemical and gas filtration, protective cloth and air filtration, etc. Antimicrobial agents which are used in industrial purposes have included quaternary ammonium salts, metal salts solutions, and antibiotics. Unfortunately, some of these agents are toxic or of poor effectiveness, which makes them not suitable for application in health foods, filters, and textiles, and for the exclusion of pollution. Among nanoparticles used for these purposes, the metallic nanoparticles are considered the most promising as they contain remarkable antibacterial properties due to their large surface area to volume ratio, which is of interest for researchers due to the growing microbial resistance against metal ions, antibiotics, and the development of resistant strains. Thus, the incorporation of nanoparticles into polymer nanofiber attracts the interest of researchers who work in biomaterial and drug delivery fields. Different types of nanomaterials like copper, zinc, titanium, magnesium, gold, alginate and silver have been developed but silver

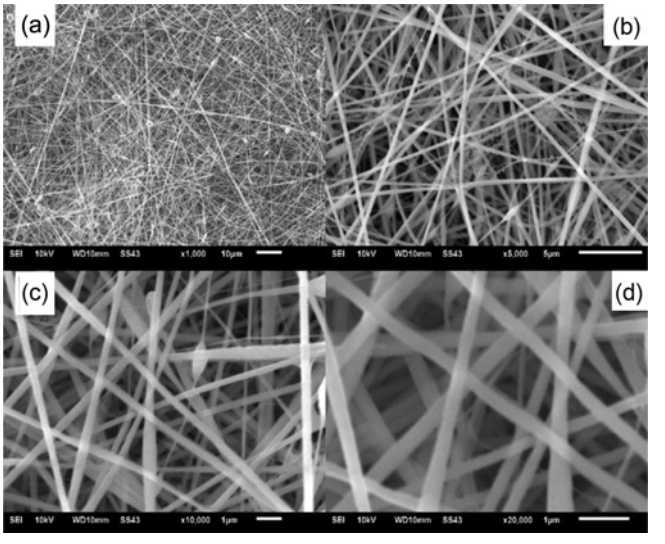

Figure 4. SEM results for Ag/PAN at (a) ×1000, (b) ×5000, (c) ×10000, and (d) ×20000.

nanoparticles (Ag NPs) have proved to be most effective as they exhibit potent antimicrobial efficacy against bacteria, viruses and eukaryotic micro-organisms. Ag NPs is used as a disinfectant drug.

The morphology of electrospun nanofibers was observed using field emission scanning electron microscope (JEOL-JSM-7600F) and scanning electron microscope (JEOL-JSM-6610 LV). Figure 4 shows SEM images of the nanofibers that were synthesized by electrospinning. These nanofiber composites were randomly oriented with their lengths extending to several micrometers.

Stabilization and Calcination of PAN/Ag Nanofibers

The electrospun PAN nanofiber bundle could be easily peeled from the aluminum foil after being immersed in distilled water. The stabilization and low-temperature carbonization were conducted in a tube furnace. A constant flow of air was maintained through the furnace during the stabilization. Prior to stabilization, the peeled electrospun PAN nanofiber bundle was dried and then tightly wrapped onto a glass rode with diameter of 2 cm; therefore, tension existed in a certain degree during the stabilization. The stabilization was carried out by heating the wrapped PAN nanofiber bundle from the room temperature to 270 °C with the heating rate set at 2 °C/min, followed by holding the temperature at 270 °C for 2 h to allow the stabilization to complete.

Figure 5 shows the SEM micrographs of the PAN/Ag fibers after calcination process at 1000 °C. From the picture we could see that nanofiber membranes were bent and twisted partly, and were not linear in structure. It was seen from the fibrous surface which was very rough as a reason to presence of a few silver nanoparticles on the fibrous surface. The PAN precursor nanofibers in the as-electrospun bundle were uniform without microscopically identifiable beads and/or beaded nanofibers [48-57]. The fiber diameters were increased slightly after calcination to be approximately 600 nm may be due to expansion of the PAN nanofibers and the distortion as a result of burning.

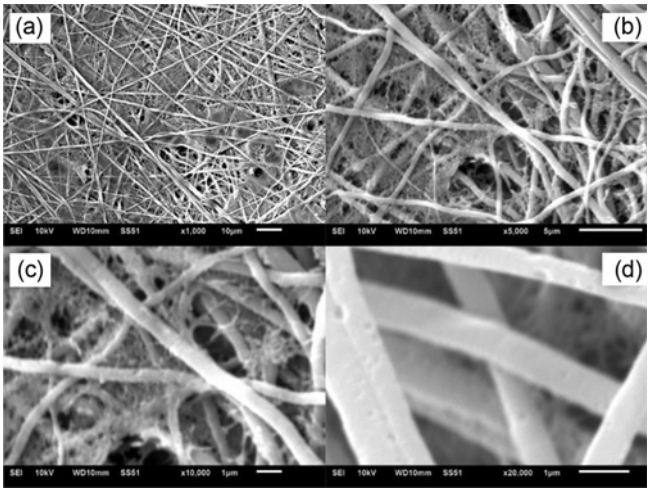

Figure 5. SEM results for PAN/Ag carbon nanofiber after calcination with different magnifications (a) ×1000, (b) ×5000, (c) ×10000, and (d) ×20000.

Although most PAN/Ag nanofibers were aligned along the rotational direction, the overall diameters of nanofiber bundle were perfect. The morphologies of the stabilized and carbonized PAN/Ag nanofibers were similar to those of the as-electrospun nanofibers except for discrepancies in diameters. The average diameter of the stabilized PAN nanofibers appeared to be almost the same as that of the as-electrospun nanofibers with little increase de to distortion. During stabilization, the PAN macromolecules in the as-electrospun nanofibers absorbed oxygen from air and went through chemical changes that resulted in cyclization of PAN macromolecules and led to formation of a ladder like polymeric structure, which no longer melted and therefore could retain the fiber morphology in the subsequent carbonization. The stabilized nanofiber bundle was subsequently un-wrapped and then carbonized at a relatively low temperature of 1000 °C in an inert (high purity nitrogen gas) environment with the heating rate set at 2 °C/min. All of the carbonized PAN nanofiber bundles were held at the respective final temperatures for 1.5 h to allow the carbonization to complete. The average diameters of the 1000 °C carbonized PAN nanofibers were 600 nm. During carbonization, a variety of gases (e.g., H_2O, N_2, HCN, and others) were evolved and the carbon content increased to 90 wt.% or higher; the process therefore led to increase in fiber diameter and the formation of three-dimensional carbonaceous structures.

The range of particle size at different angles shown in Figure 6. Thermal properties of electrospinning nanofibers were examined through using thermogravimetric analysis TGA (Figure 7) which were carried on TA-Q500 System of TA; samples of 5-10 mg were heated in the temperature range 30-800 °C at a scanning rate of 10 °C·min^{-1} under nitrogen atmosphere, and by using TG-DTA: NETZSCH germany (Model: STA 449 F_3). While the bonding

Unimodal Results Summary

Angle	Mean (nm)	P.I.	Diff.Coef (m²/s)	Counts/s	Baseline Error	Overflow
10.2°	11.2	-12.214	1.59e-11	1.58e+06	0.04%	0
27.5°	16.9	0.840	1.05e-11	2.36e+06	0.07%	0
90.0°	67.5	1.490	2.63e-12	2.25e+06	0.08%	0

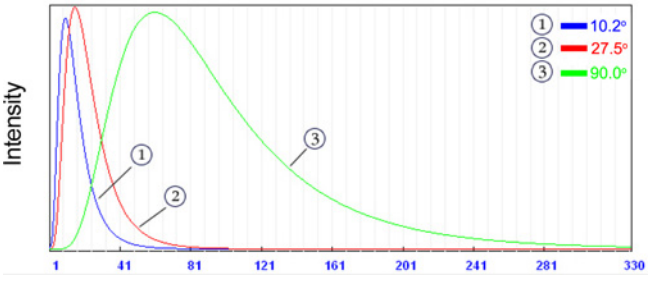

Figure 6. Particle size for Ag.

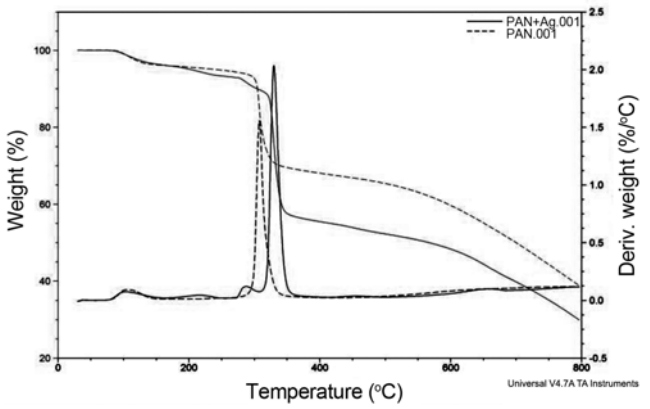

Figure 7. TGA results for Ag/PAN.

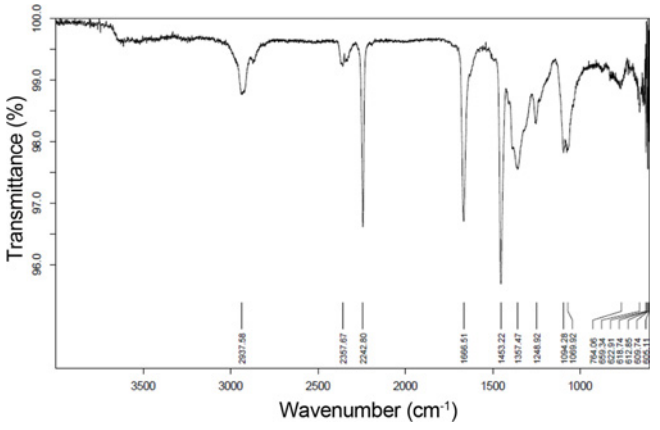

Figure 8. FTIR results for Ag/PAN.

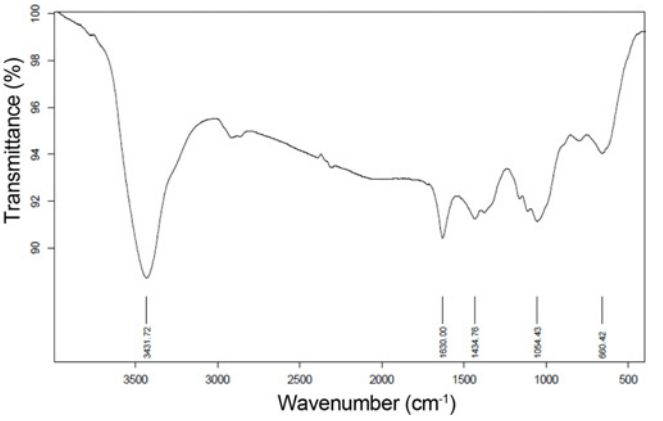

Figure 9. FTIR results for Ag/carbon nanofibers.

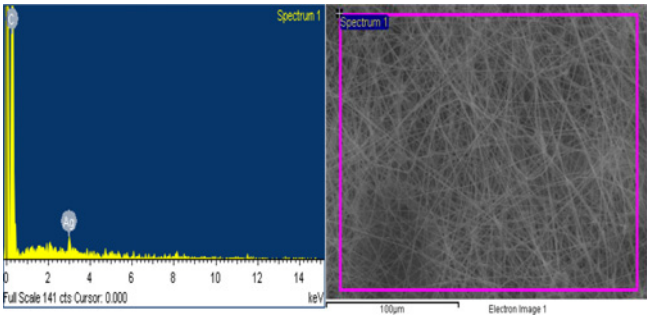

Figure 10. EDS analysis of carbon nanofiber confirms the presence of Ag in PAN matrix.

configurations of the samples of carbon nanofibers were characterized by Fourier-transformer infrared (FT-IR) Spectra (Figure 8) were recorded using TENSOR 27, Bruker. Generally PAN begins to degrade when heated near its melting point. The degradation reaction of PAN is so exothermic that it tends to obscure its melting endotherm in ordinary DSC traces. Therefore, the melting endotherm is normally not observed in PAN. In this study, DSC and DTA were conducted in N_2 atmosphere as shown in Figure 7.

There is one sharp exothermic peak at 295 °C for electrospun fibers. It has been reported that an exothermic reaction ranging between 200 and 350 °C in an inert atmosphere is typical of PAN/Ag. The peak is attributed to the cyclization of the nitrile groups of PAN. However, the peak shifts to lower temperature for electrospun fibers. The shift of exothermic onset peak to low temperature suggests that cyclization is more easily initiated at low temperature for electrospun fibers. Molecular chains were oriented within the electrospun fibers during the electrospinning process. On the other hand, the shift may be attributed to the large conductivity of electrospun fibers. The detailed mechanism of the shift will be studied further.

Figure 8 reveals typical FT-IR spectra for the PAN nanofibers. The vibrations characteristics of the PAN structure are similar to those reported in Figure 9 for PAN/Ag nanofibers. The only change that the bands are relatively shifted little bet higher due to high conductivity of the PAN/Ag nanofibers.

The energy dispersive spectrum (EDS) collected on the PAN/Ag NPs sample (whose microstructure is illustrated in Figure 4) distinctly identifies Ag as the elemental component in the fiber and is shown in Figure 10. The other peaks belonging to carbon are generated from the PAN. Elementary analysis of PAN/Ag NPs nanocomposite was carried out by using SEM-EDS. The results show that carbon and Ag were the principal element of PAN/Ag NPs nanocomposite. EDS analysis thus provides direct evidence that Ag ions embedded in the PAN/silver nanocomposite. It is indicated that silver nanoparticles were well loaded without any chemical and structural modifications into PAN polymer matrix to form an organic-inorganic nanocomposite.

The presence of silver formation after drying was confirmed by XRD as shown in (Figure 11). The nanofibers exhibited two equatorial peaks with a diffuse meridian peak. The primary equatorial $(10\bar{1}0)$ peak at $2\theta=16.88$ ° corresponds to a spacing of d=5.25 Å while the weaker reflection $(11\bar{2}0)$ at $2\theta=29.5$ ° corresponds to a spacing of d=3.05 Å (note Miller

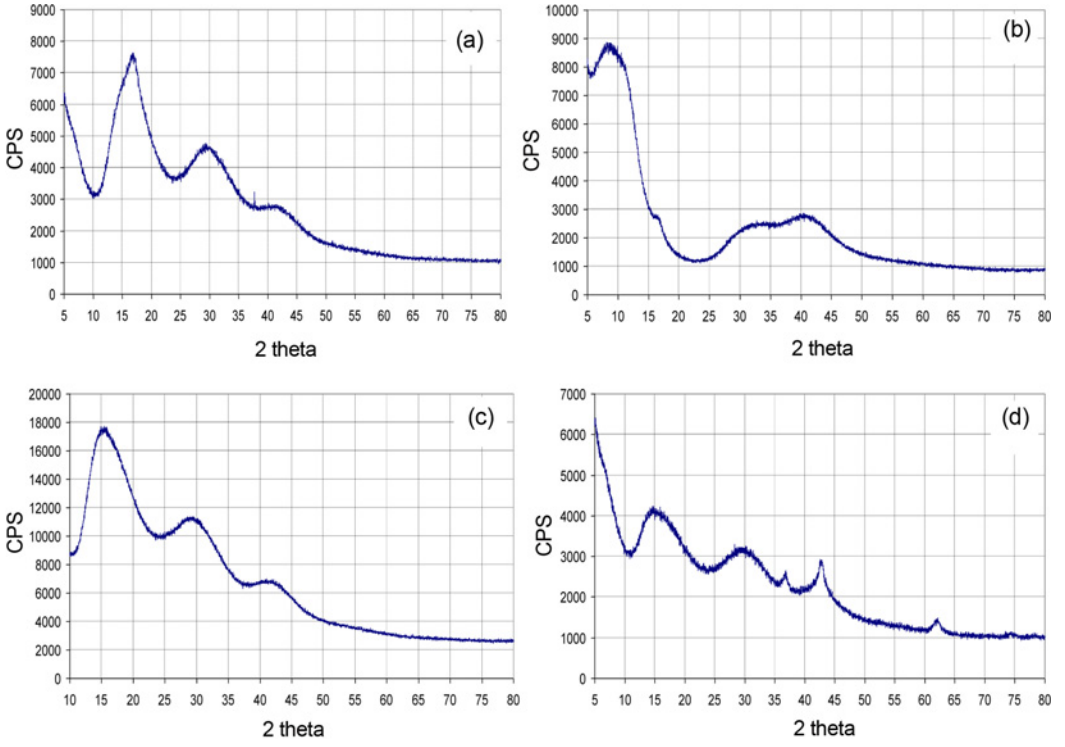

Figure 11. XRD results for (a) pure PAN, (b) Ag PAN, (c) pure PAN after calcination, and (d) Ag PAN after calcination.

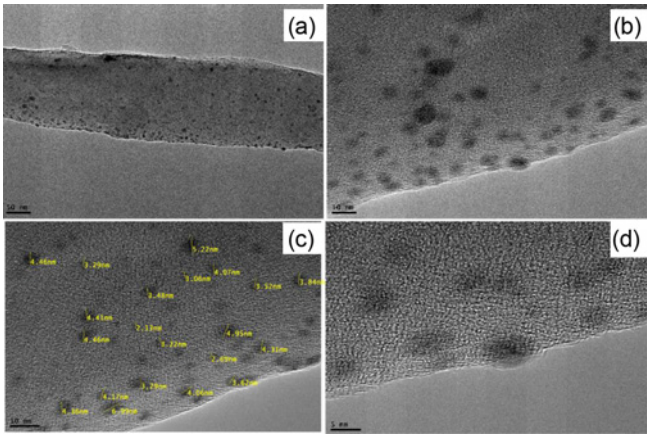

Figure 12. TEM results for Ag/PAN; (a) 50 nm, (b) 10 nm, (c) Ag particles sizes, and (d) 5 nm.

indices (hkil) are used for identification of planes in hexagonal crystals).

TEM images were obtained with a model JEOL JEM-2010 FEF operating at 200 kV. Figure 12 showed Ag nanoparticles (seen as black phase) were spherical in shape and encapsulated in translucent PAN. It is also shows how the embedding of Ag nanoparticles into these nanofibers to form composite. Many factors influence the diameters and morphology of the electrospun nanofibers, such as solution concentration, applied voltage, solution velocity, tip-to-collector distance, and solution properties (polarity, surface tension, electric conductivity, etc.). From the TEM images, individual silver nanoparticles were examined using the field emission transmission electron microscope (JEOL-JEM-2100F, Japan), it is observed to be homogeneously distributed within the fiber matrix, and no significant aggregation was observed. While the NF (Figure 5(a)) had a smooth surface without any particles, the silver nanoparticles were all spherical, and their average size decreased from 20 to 10 nm (Figure 12(c)).

Table 1. Inhibition zone of foodborne pathogens

Strains/Samples	Inhibition zone diameter (mm) 2×10^6	
	PAN	PAN/Ag
Bacillus cereus	6	8
Staphylococcus aureus	No zone of inhibition observed	8
E.coli o157:H7	No zone of inhibition observed	8

Antibacterial Activities (Preliminary Results)

The 4 samples showed various degrees of inhibition against the 3 bacteria strains using the disc diffusion method as presented in Table 1. Sample with an enhanced inhibitory effect was PAN/Ag nanofibers which inhibited all strains (inhibition zone diameter 8 mm); sample pure PAN nanofibers inhibited one strain (*Bacillus cereus*) with zone diameter 6 mm.

Conclusion

Polyacrylonitrile (PAN) in its compositing with silver nanoparticles (AgNPs) was successfully prepared in the form of nanofibrous membranes by electrospinning. The simultaneous one-pot synthesis of Ag/NF composites has several advantages in terms of controlling particle size and fiber diameter. The resulting solution was electrospun into ultrafine NF composites. In addition, the FTIR spectroscopy, thermal gravimetry analysis (TGA) proved the presence of silver nanoparticles in the PAN fiber. The SEM micrographs clarified that there are random orientation for nanofiber. Fibrous membranes with antibacterial activity were prepared from 5 % w/v polyacrylonitrile (PAN) solutions containing silver nitrate ($AgNO_3$) in the amounts of 0.5-2.5 % by weight of PAN by electrospinning. N,N Dimethylformamide (DMF) was used as both the solvent for PAN and reducing agent for Ag ions. The enhancement in the reduction process was achieved with UV irradiation, which resulted in the formation of larger AgNPs in areas adjacent to and at the surface of the fibers. Without the UV treatment, the size of the AgNPs was smaller than 5 nm on average. Under the 10 min of UV treatment, the size of the particles increased with an increase in the initial $AgNO_3$ concentration in the solutions to range between 5.3 and 7.8 nm on average. Without or with the UV treatment, the diameters of the obtained PAN/AgNPs composite fibers decreased with an increase in the initial $AgNO_3$ concentration in the solutions, with the diameters of the obtained composite fibers that had been subjected to UV irradiation exhibiting lower values (i.e., 185-205 nm versus 194-236 nm on average). Both the cumulative amounts of the released silver and the bactericidal activities of the PAN/AgNPs composite fibrous materials against two commonly-studied bacteria, i.e., Gram-positive Staphylococcus aureus and Gramnegative Escherichia coli, increased with increases in both the initial $AgNO_3$ concentration in the solutions and the UV irradiation time interval.

Acknowledgement

This work was financially supported by the National Plan for Science & Technology (NPST), King Saud University Project No. 11-NAN1460-02.

References

1. D. Y. Lee, K.-H. Lee, B.-Y. Kim, and N.-I. Cho, *J. Sol-Gel Sci. Technol.*, **54**, 63 (2010).
2. C. Zhang, Q. Yang, N. Zhan, L. Sun, H. Wang, Y. Song, and Y. Li, *Colloids and Surfaces A: Physicochem. Eng. Aspects*, **362**, 58 (2010).
3. Y. Wang, Q. Yang, G. Shan, C. Wang, J. Du, S. Wang, Y. Li, X. Chen, X. Jing, and Y. Wei, *Mater. Lett*., **59**, 3046 (2005).
4. P.-O. Rujitanaroj, N. Pimpha, and P. Supaphol, Wiley InterScience DOI 10.1002/app.31498 (2010).
5. L. Francis, F. Giunco, A. Balakrishnan, and E. Marsano, *Synthesis*, *Current Appl. Phys.*, **10**, 1005 (2010).
6. J. Bai, Q. Yang, S. Wang, and Y. Li, *Korean J. Chem. Eng*., **28**, 1761 (2011).
7. H. H. Chae, B.-H. Kim, K. S. Yang, and J. I. Rhee, *Synthetic Metals*, **161**, 2124 (2011).
8. P. Jain and T. Pradeep, *Biotechnol. Bioeng*., DOI: 10.1002/bit.20368 (2011).
9. B. Bagheri, M. Abdouss, M. M. Aslzadeh, and A. M. Shoushtari, *Iranian Polym. J.,* **19**, 911 (2010).
10. M. S. A. Rahaman, A. F. Ismail, and A. Mustafa, *Polym. Degrad. Stab.,* **92**, 1421 (2007).
11. L. Kriklavova and T. Lederer, *Proc. 3rd Int. Conf. NANOCON* (2011).
12. D. K. Tiwari, J. Behari, and P. Sen, *World Appl. Sci. J.,* **3**, 417 (2008).
13. G. R. Kiani, H. Sheikhloie, and N. Arsalani, *Desalination,* **269**, 266 (2011).
14. C. J. Thompson, G. G. Chase, A. L. Yarin, and D. H. Reneker, *Polymer*, **48**, 6913 (2007).
15. D. Esrafilzadeh, M. Morshed, and H. Tavanai, *Synthetic Metals*, **159**, 267 (2009).
16. S. N. Arshad, M. Naraghi, and I. Chasiotis, *Carbon,* **49**, 1710 (2011).
17. L. Kriklavova and T. Lederer, *Proc. 4th Int. Conf. NANOCON* (2012).
18. K. Tiwari, J. Behari, and P. Sen, *World Appl. Sci. J.*, **3**, 417 (2008).
19. R. Balamurugan, S. Sundarrajan, and S. Ramakrishna, *Membranes*, **1**, 232 (2011).
20. B. Bagheri, M. Abdouss, M. Aslzadeh, and A. Shoushtari, *Iranian Polym. J.*, **19**, 911 (2010).
21. G. Kiani, H. Sheikhloie, and N. Arsalani, *Desalination*, **269**, 266 (2011).
22. D. Shao, Q. Wei, L. Zhang, Y. Cai, and S. Jiang, *Appl. Surf. Sci.*, **254**, 6543 (2008).
23. C. Thompson, G. Chase, A. Yarin, and D. Reneker, *Polymer*, **48**, 6913 (2007).
24. Z. Zhou, C. Lai, L. Zhang, Y. Qian, H. Hou, D. Reneker, and H. Fong, *Polymer*, **50**, 2999 (2009).
25. L. Kriklavova and T. Lederer, *Proc. 2nd Int. Conf. NANOCON* (2010).
26. Y. Tong, X. Wang, H. Su, and L. Xu, *Corrosion Science*, **53**, 2484 (2011).
27. M. Rahaman, A. Ismail, and A. Mustafa, *Polym. Degrad. Stab.*, **92**, 1421 (2007).
28. M. Yu, Y. Bai, C. Wang, Y. Xu, and P. Guo, *Mater. Lett*., **61**, 2292 (2007).
29. D. Esrafilzadeh, M. Morshed, and H. Tavanai, *Synthetic Metals*, **159**, 267 (2009).
30. X. Hou, X. Yang, L. Zhang, E. Waclawik, and S. Wua,

Materials and Design, **31**, 1726 (2010).
31. C. Su, Z. Jiang, and C. Lu, *Fiber. Polym.*, **13**, 38 (2012).
32. H. Wang, P. Gao, S. Lu, H. Liu, G. Yang, J. Pinto, and X. Jiang, *Electrochimica Acta*, **58**, 44 (2011).
33. H. Zhang, H. Nie, D. Yu, C. Wu, Y. Zhang, C. Branford, and L. Zhu, *Desalination*, **256**, 141 (2010).
34. S. Arshad, M. Naraghi, and I. Chasiotis, *Carbon*, **49**, 1710 (2011).
35. P. Neghlani, M. Rafizadeh, and F. Taromi, *J. Hazard. Mater.*, **186**, 182 (2011).
36. S. Moon and R. Farris, *Carbon*, **47**, 2829 (2009).
37. K. Lee, N. Shiratori, G. Lee, J. Miyawaki, I. Mochida, S. Yoon, and J. Jang, *Carbon*, **48**, 4248 (2010).
38. Y. Wang, Q. Yang, G. Shan, C. Wang, J. Du, S. Wang, Y. Li, X. Chen, X. Jing, and Y. Wei, *Mater. Lett*., **59**, 3046 (2005).
39. P. Rujitanaroj, N. Pimpha, and P. Supaphol, *J. Appl. Polym. Sci.*, **116**, 1967 (2010).
40. L. Francis, F. Giunco, A. Balakrishnan, and E. Marsano, *Current Appl. Phys.*, **10**, 1005 (2010).
41. D. Lee, K. Lee, B. Kim, and N. Cho, *J. Sol-Gel Sci. Technol.*, **54**, 63 (2010).
42. K. Juengsuwattananon, P. Rujitanaroj, P. Supaphol, N. Pimpha, and S. Matsuzawa, *Mater. Sci.*, **569**, 25 (2008).
43. J. Bai, Q. Yang, S. Wang, and Y. Li, *Korean J. Chem. Eng*., **28**, 1761 (2011).
44. W. Zhang, Y. Wang, and C. Sun, *J. Polym. Res.*, **14**, 467 (2007).
45. C. Su, Z. Jiang, and C. Lu, *Fiber. Polym.*, **13**, 38 (2012).
46. C. Teh and A. Mohamed, *J. Alloy. Comp.*, **509**, 1648 (2011).
47. D. Tiwari, J. Behari, and P. Sen, *World Appl. Sci. J.*, **3**, 417 (2008).
48. T. Amna, M. Hassan, N. Barakat, D. Pandeya, S. Hong, M. Khil, and H. Kim, *Appl. Microbiol. Biotechnol.*, **93**, 743 (2012).
49. H. Chae, B. Kim, K. Yang, and J. Rhee, *Synthetic Metals*, **161**, 2124 (2011).
50. H. Bai, Z. Liu, and D. D. Sun, *Applied Catalysis B: Environmental*, **111-112**, 571 (2012).
51. L. Zhang, J. Luo, T. Menkhaus, H. Varadaraju, Y. Sun, and H. Fong, *J. Membr. Sci.*, **369**, 499 (2011).
52. P. Jain and T. Pradeep, *Biotechnol. Bioeng.*, **90**, 59 (2005).
53. M. Seery, R. George, P. Floris, and S. Pillai, *J. Photochem. Photobiol. A: Chemistry*, **189**, 258 (2007).
54. M. Kanjwal, N. Barakat, F. Sheikh, W. Baek, M. Khil, and H. Kim, *Fiber. Polym.*, **11**, 700 (2010).
55. D. Huyen, N. Tung, N. Thien, and L. Thanh, *Sensors*, **11**, 1924 (2011).
56. Y. Li, M. Ma, W. Chen, L. Li, and M. Zen, *Mater. Chem. Phys.*, **129**, 501 (2011).
57. G. Sichani, M. Morshed, M. Amirnasr, and D. Abedi, *J. Appl. Polym. Sci*., **116**, 1021 (2010).